

Article

Assessment of the Possibility of Application of New Types of Filler Materials in the Renovation of Functional Surfaces of Crane Wheels

Ján Viňáš^{1,*} , Janette Brezinová² , Peter Horňák³ , Jakub Brezina¹, Peter Pinke⁴ and Tünde Anna Kovács⁴ 

¹ Department of Technology, Materials and Computer Aided Production, Faculty of Mechanical Engineering, Technical University of Košice, 042 00 Košice, Slovakia; jakub.brezina@tuke.sk

² Department of Automotive Production, Faculty of Mechanical Engineering, Technical University of Košice, 042 00 Košice, Slovakia; janette.brezinova@tuke.sk

³ Institute of Materials and Quality Engineering, Faculty of Materials, Metallurgy and Recycling, Technical University of Košice, 042 00 Košice, Slovakia; peter.hornak@tuke.sk

⁴ Bánki Donát Faculty of Mechanical and Safety Engineering, Óbuda University, Népszínház u. 8., H-1081 Budapest, Hungary; pinke.peter@bgk.uni-obuda.hu (P.P.); kovacs.tunde@bgk.uni-obuda.hu (T.A.K.)

* Correspondence: jan.vinas@tuke.sk

Abstract: This paper presents the results of research from the renovation of functional parts of crane wheel surfaces. The aim of the research was to verify the possibilities of changing the chemical composition of the additive materials for submerged arc cladding, in order to increase the resistance of the wheel surfaces to wear. The base material of the crane wheel was heat-treated carbon steel for castings, mat. no. 1.0553. The renovation process was carried out on three equal wheels. Conventionally used additive material, the same one used for the interlayer and two covering layers, was used on one wheel. On two other wheels, newly increased tubular wires with a higher proportion of carbide-forming additives (Cr, Mo) were used for the carbide coating of two covering layers, in addition to their conventional additive material. Low-alloy additive material was applied to the newly elevated wires. The quality of the clads was assessed using non-destructive tests. Subsequently, microstructural analysis was carried out on the test samples taken from the renovated wheels, by means of light microscopy. On the cross cuttings, the course of hardness was evaluated using Vickers analysis. The resistance of functional surfaces to adhesion wear was evaluated based on weight losses measured using the AMSler experimental equipment. The results of the experiments showed an increase in the tribological resistance of the surfaces, specifically by 45% due to the newly developed wire C1 and by 18% due to wire B1, and it is therefore possible to recommend renovation.

Keywords: cladding; wheel; renovation



Citation: Viňáš, J.; Brezinová, J.; Horňák, P.; Brezina, J.; Pinke, P.; Kovács, T.A. Assessment of the Possibility of Application of New Types of Filler Materials in the Renovation of Functional Surfaces of Crane Wheels. *Metals* **2024**, *14*, 1185. <https://doi.org/10.3390/met14101185>

Academic Editor: Slobodan Mitrovic

Received: 12 August 2024

Revised: 17 September 2024

Accepted: 26 September 2024

Published: 18 October 2024



Copyright: © 2024 by the authors. Licensee MDPI, Basel, Switzerland. This article is an open access article distributed under the terms and conditions of the Creative Commons Attribution (CC BY) license (<https://creativecommons.org/licenses/by/4.0/>).

1. Introduction

In primary metallurgical production, especially in heavy engineering, travelling cranes play an extremely important role. Chovnyuk, Y. et al. and Chen, K., in their works [1,2], presented current design solutions for bridge cranes. These cranes allow for the manipulation and transport of minerals, molten metals, semi-finished products and finished products. Their design is different depending on their load capacity, which ranges from one to several hundred tons. A number of factors and input variables influence the overall load capacity of cranes, which were clearly defined by Wang, R.D. et al. [3]. In [4], Olearczyk, J. et al. addressed the possibilities of implementing modular design systems while speeding up the overall design process. In particular, the field of metallurgical production, especially iron and steel production, requires the greatest load-bearing capacity to handle the products. The movement of these cranes is carried out during operations by means of steel crane wheels, which are located on rails. These are tandem wheels on each side of the crane, but, due to the constant requirement to increase production efficiency and the amount of goods

transported, there is pressure to increase their load-bearing capacity. To solve this, a new design is proposed, incorporating more than 10 travelling wheels on each side of the crane, allowing for a better distribution of forces on the track. These travelling rails may also vary significantly during their construction. Many different types of software can be used in the design of cranes, but it is very important that these software implement as many relevant input variables as possible, in order to minimize the error rate of the resulting designs. Interesting results on the use of these software have been published by Quang Huy Tran et. al. in [5], in which they defined the error rate using the capacitance spectrum method (CSM) and the equivalent linearization method (ELM). The strength calculations required for the design of cranes must also take into account secondary factors that may cause their destruction. It is certainly not good to forget, for example, the weather as a factor, which, when handling loads, can fundamentally change the impact of the overall load on the structure, as pointed out in the work of Tang, G. et al. [6]. Due to their handling and relocation of heavy loads, these technically complex devices have a limited lifetime [7–9]. The conditions of their operation are defined in strict directives, as, in emergencies, cranes can cause considerable economic damage and potentially the loss of human lives. Therefore, regular inspections are prescribed and necessary to eliminate all possible risks [10]. During the crane's operation, it is necessary to regularly check the statuses of lifting devices, including ropes, as well as the condition of the anchoring parts, which include hooks, some of the pulleys and the reel fastenings [11]. However, the most burdened crane elements are, without contest, the crane wheels [12]. Their limited lifetime is due to a number of factors, of which tribodegradation factors are primary. This includes combined adhesive–abrasive wear. This type of wear is created through the interaction of the steel surface and the steel rail, especially when the crane is braking. Its intensity depends on operating conditions, taking into account the surrounding environment, but also on the method of operation. Often, the operator affects the intensity of this tribodegradation process through their use of the crane, e.g., intense stopping and braking. This abrasive wear increases the amount of impurities on the crane path and produces dust during operation [13,14]. This issue is especially topical in the context of metallurgic production. There are no necessary additional technological measures in the form of cleaning elements on cranes that ensure the minimization of the occurrence of dirt on the crane's path. In the event of damage to the surface of even one wheel in the wheel system, the surface delamination and subsequent separation of particles from the wheel can cause damage to the other wheels in the system [15,16]. It is therefore advisable to carry out wheel replacement throughout the system, on all wheels. Another degradation factor is surface corrosion. As travelling cranes work predominantly under the roof in these types of operations, there is an accumulation of matter, fume condensation, etc. The rolling of surfaces along the same path continually can also cause fatigue wear. Research on the influence of these dynamic effects, based on precise measurements of rail deformations as well as sensors in the wheels, has been published by Kettler et al. in their paper [17], in which they established a new evaluation methodology in order to increase the accuracy of the estimation of the lifetime of cranes. The surfaces of the wheels are subjected to the effects of large amounts of pressure concentrated on a small area. The impact of secondary degradation factors increases when cranes are overloaded, especially in conditions where there are no other safety features preventing them from overloading. The action of large amounts of pressure on damaged surfaces can cause cracking, which can lead to a fragile wheel fracture. The most frequently observed type of damage to the wheel surface is this so-called mapping (cracking) of the surface and the subsequent break-up of wheel segments. This is already a critical state. The faces of crane wheels can be made of moulded or forged semi-finished products, but the bulk of the wheels is produced through casting. The material for production is used to create a casting, the chemical composition of which varies depending on the manufacturer. The lifetime of the wheels is limited by the conditions under which they operate and also the materials used for their production. Their condition should be regularly checked. In the event of damage to their functional surfaces, namely the rims, which ensure the correct position

of the wheel on the crane track and prevent its deviation from the track, it is necessary to remove such a crane from operation and replace the wheels. Currently, surface renovation is a highly topical issue in renovation technologies, especially from the point of view of material savings, especially for large amounts (up to several tonnes) of components, and also for components made of materials with specific alloy requirements [18,19]. Methods such as MMAW and GTAW can be used for local repairs of the damaged surface. Even for local repairs, it is necessary to consistently follow all technological measures necessary for their implementation. This includes, in particular, a suitably chosen preheating treatment and subsequent heat treatment for the renovated wheels. Preheating must be applied to prevent the formation of cold cracks caused by unsuitable hard structures as well as internal residual stresses. However, local wheel repairs are not frequent. Much more common are repairs of the entire functional part of the wheel. Based on the assessment of the extent of the damage to the wheel removed from the operation and of the treatments to control for the presence of cracks, the damaged parts from the wheels are removed using chip machining. This can constitute a turning or milling method. The condition of the hole for storing the bearing in the wheel is also checked. After the chip machining, the wheel is ready for automated cladding-based renovation. This is carried out by cladding around the perimeter of the wheel, which is preheated to the desired temperature, ensuring its smooth rotation corresponding to the cladding speed used in the given technology. The diameters of wheels measuring up to 200 mm are renovated using the GMAW and FCAW methods. Wheels with average diameters of above 200 mm can be renovated using SAW cladding. Non-flammable bonds, which prevent the cladding from melting and thus revealing the arc, are used at the cladding site. Immediately after this, the wheels are placed in lining pots filled with perlite, before being placed into annealing furnaces, where they slowly cool. This part of the renovation requires high attention and compliance with all technological measures. The cooling must be slow and evenly distributed.

This paper presents the results of research aimed at optimizing the process of renovation of mobile crane wheels and verifying the possibility of applying a new type of additive material for cladding. The reason for the innovation of the chemical composition of the additive materials was to verify the possibilities of increasing the resistance of the contact surfaces of the wheel when using additive elements by allowing the formation of finely dispersed carbide compounds in the base structure of the wheels.

2. Materials and Methods

The extent of damage (Figure 1) was assessed on the crane wheel. The documented wheel had a dimension of $\varnothing 950 \text{ mm} \times 180 \text{ mm}$. As the presence of cracks was not observed, the wheel was intended for renovation. The travel wheel intended for renovation was made of carbon steel for castings. The 1.0553 chemical composition of the steel type for castings detected by the spectral Chemical Analyzer Belec Compac Port (Belec Spektrometrie Opto-Elektronik GmbH, Georgsmarienhütte, Germany) is shown in Table 1. The mechanical properties of the steel are shown in Table 2.

Depending on the application and working conditions, different geometries of wheels can be distinguished:

- Wheel without rims;
- Wheel with a single rim;
- Wheel with two rims;

as well as the two main types of contact surface:

- Conical;
- Cylindrical.

The crane wheel was in an interaction with the JKL100 rail made of R260 EN 13674-4 [20], with the load capacity of the crane being twenty tons. The hardness of the rail material was 240–260 HV. The shape and dimensions of the wheel after the renovation are presented in Figure 2. Several tribodegradation factors affected the service life of the travel wheels at

the same time. Primarily, this was wear and even the side rim breakage; another frequent factor was the focus of the bearings, the failure of the axle, or the crane cross and the wear of the surfaces.

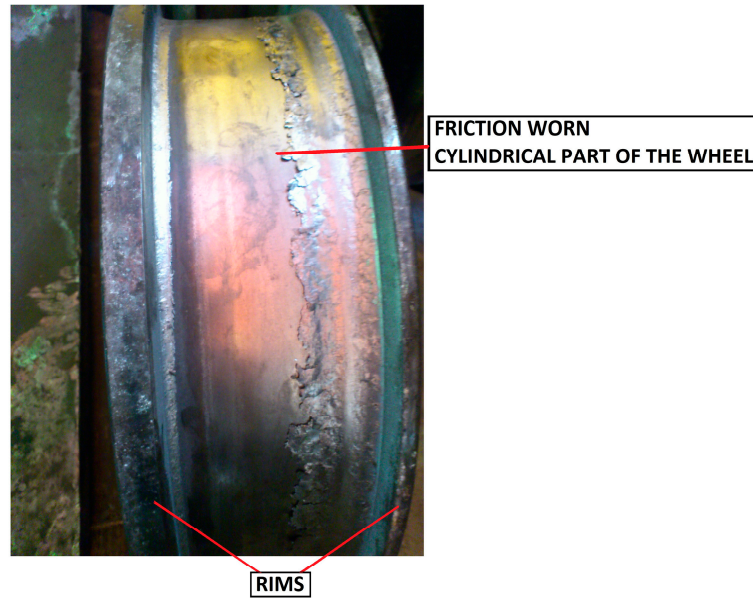


Figure 1. Worn-out wheel intended for renovation.

Table 1. Chemical composition of the base material mat. no. 1.0553 (wt.%).

C	Mn	Si	P	S	Cr	Ni	Mo	V	Cu	Fe
0.46	0.62	0.380	0.009	0.008	0.006	0.099	0.011	0.004	0.016	Bal.

Table 2. Mechanical properties of the base mat. no. 1.0553 by manufacturer.

Yield Strength (MP(a))	Tensile Strength (MP(a))	Hardness HB
300	590–740	170–210

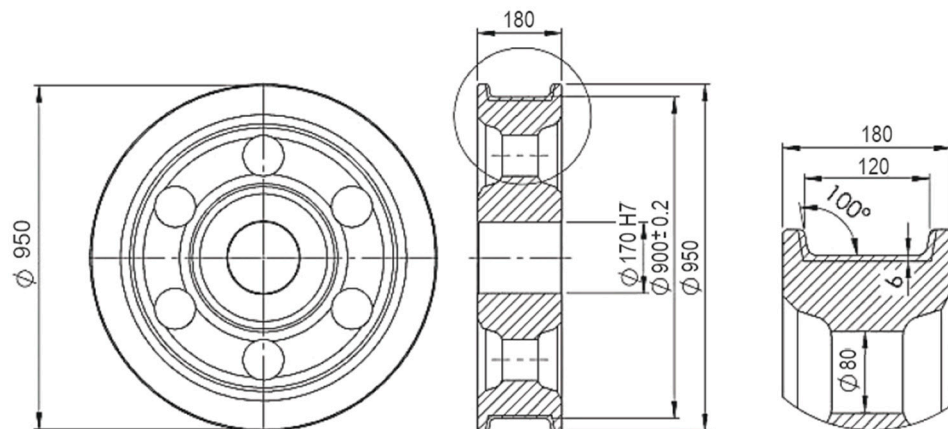


Figure 2. Dimensions of the crane wheel intended for renovation.

The renovation process consisted of assessing the condition of wear of the functional surfaces of the wheel. Visual inspection assessed the extent of damage. The aim of the inspection was to identify the occurrence of cracks on the functional surfaces of the wheel.

After the inspection, the wheel was machined by turning. If the crane wheel had been renovated, it would be possible to remove the previous clad on the crane wheel. The thickness of the layer of the material removed is different for each wheel depending on the size of the wheel damage. By default, the machine was removed to a depth of 10 mm to the wheel diameter at the point of the horizontal contact area. After the chip processing, the process of renovation was carried out by cladding. The renewal of functional surfaces was carried out by the cladding technology under melt. Three types of additive types of conventional type of cladding wire labeled A1, which was used as a standard, were used for the cladding of the wheel surfaces. The newly developed wires designed to produce the cover layers were marked as B1 and C1. In the production of clads using new types of wires, the interlayer was applied, which was made by a D1 wire. The chemical compositions of the individual cladding wires used during the experiment are defined in Table 3. As part of the experiments, three types of wire for cladding under the melt were used. Their chemical composition is defined in Table 4.

Table 3. Chemical composition of the filler material (in wt.%) (Fe balance).

Wheel	Layer	WM	C	Mn	Si	Cr	Mo	Ni	Al	Cu	Flux
w01	CL	A1	0.3	1.0	0.1	1.0	-	-	-	-	F1
	IL	A1	0.3	1.0	0.1	1.0	-	-	-	-	F1
w02	CL	B1	0.32	1.1	0.6	2.9	0.9	-	-	-	F3
	IL	D1	0.07–0.15	0.8–1.3	0.11	-	-	-	-	max. 0.3	F2
w03	CL	C1	0.2	0.9	0.8	4.8	0.5	0.5	0.5	-	F3
	IL	D1	0.07–0.15	0.8–1.3	0.11	-	-	-	-	max. 0.3	F2

Note(s): CL—cover layer; IL—interlayer; w01–w03—marking for cladded wheels.

Table 4. Used agglomerated flux [21].

Flux	F1	F2	F3
Classifications	DIN 32522: BAR 197 AC 8 SMK 2-16	DIN 32522: FMS 188 AC 8M 2-16	DIN 32522: BAB 167 AC 8M HP5 2-16
Slag type	Aluminate–rutile	Manganese–silica	Aluminate–basic
Density	1.2 kg/dm ³	1.5 kg/dm ³	1.2 kg/dm ³
Basicity index	0.6	0.7	1.5

2.1. The Process of Renovation of Wheels

The cladding process was carried out on the WST 1000 (from the manufacturer VUZ Bratislava, Slovakia) (Figure 3). It is a slot machine for single-arc cladding under the melt, a cladding wire with a diameter of \varnothing 2 mm to 4 mm with an alternating or direct current up to 1000 A. It allows for the rotation of surfaces with a maximum diameter of \varnothing 1200 mm and 2000 mm length. The rotary surfaces can be found in the circles around the perimeter, but the wheel is used in the screws. The device allows for the oscillation of the cladding head at a width of 40 mm. Due to the dimensions of the wheels and the thickness of the compliance areas exceeding 20 mm, as well as the chemical composition of the basic wheel material, it is necessary to apply it before and during the preheating in order for it to operate. Depending on the type of additive material used for the cladding of wheels for research, the pre-heating interval was elected from 150 to 200 °C. The pre-heat was realized in an annealing oven. During cladding, the temperature height was maintained using the propane-butane flame tandem torches. Temperature height was monitored by a testo 835-T1-4 Point Infrared Thermometer to 600 °C, producer Testo, s.r.o. Praha 5 Czech Republic. The cladding parameters used are defined in Table 5.

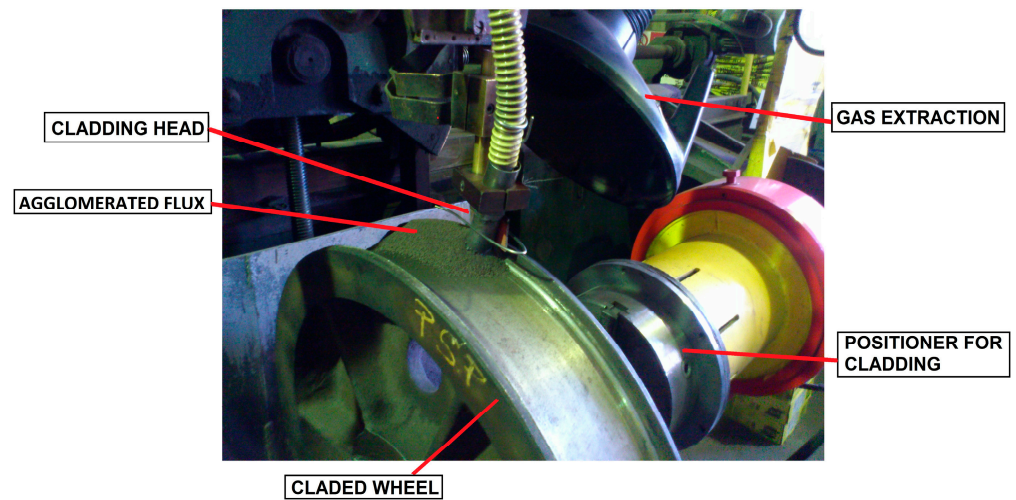


Figure 3. Cladding process on a wheel with two rims (WTS 1000).

Table 5. Used parameters of the cladding wheel.

Wheel	Layer	WM	Overlapping Layers	Current [A]	Voltage [V]	Cladding Speed [m/hod]
w01	CL	A1	½ layers	300–380	30	25
	IL	A1	½ layers	300–380	28–30	25
w02	CL	B1	1/3 layers	300–380	30	25
	IL	D1	1/3 layers	300–380	28–30	25
w03	CL	C1	1/3 layers	300–380	30	25
	IL	D1	1/3 layers	300–380	28–30	25

Note(s): CL—cover layer; IL—interlayer; used diameter of wire—ø 3.2 mm; w01–w03—marking for cladded wheels.

One interlayer and two covering layers were cladded for all wheels. The process is documented in Figure 4a,b.

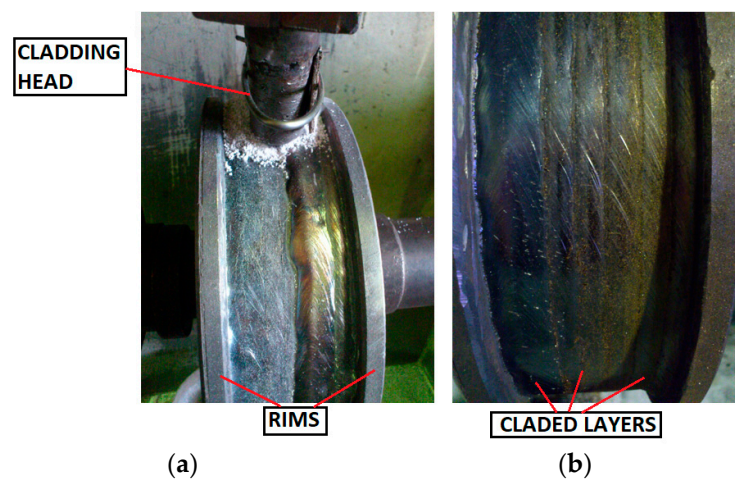


Figure 4. Renovation of the crane wheel: (a) cladding of the wheel under the melt in the screws; (b) surface of the wheel after cladding before heat treatment.

2.2. The Heat Processing of the Wheels after the Cladding

The wheel temperature at 150–200 °C intervals was maintained during the cladding. Immediately after cladding, the wheel was moved to an induction oven for isothermal annealing. The application of heat treatment to the wheels was necessary in order to reduce the size of the internal stresses introduced during fusion welding, as well as because of recrystallization and the reduction in grains in the grain structure of the filler and subfiller areas, and it was also important in order to achieve the required hardness of the functional parts of the wheels. This was followed by smooth heating to a temperature of 800–840 °C. The heating was followed by cooling in the oven to 620 °C for 2.5 h. After removing the wheels from the furnace, the wheels were cooled by the air. They were placed in the stands that prevented their contact with each other, ensuring their even cooling. After cooling, the wheels were turned to the desired dimensions.

2.3. Methods of Quality Evaluation of the Wheels After Cladding

The quality of the cladding layers was evaluated by non-destructive methods. Visual check was the first to be used. Visual control of clads was carried out in accordance with EN ISO 17637 [22] in the lighting of 500 lux. The lighting intensity was measured by the Luxmeter Testo 540 (producer Testo, s.r.o. Praha 5 Czech Republic). On the wheels, the presence of surface errors was evaluated. Errors were classified according to EN ISP 6520-1 [23]. The visual inspection was followed by a capillary control. It was realized in accordance with EN ISO 3452 [24]. The color method was applied. Diffu-Therm Bre-S (product Helmut Klumpf KG, Herten, Germany) was used to clean the surface before applying the penetration fluid in the aerosol form. As an indication fluid, the penetrant used was AE-ROSOL Diffu-Therm BDR (product Helmut Klumpf KG, Herten, Germany), a red dye aerosol. After a specified penetration time, the surface cleansing and application developers Diffu-Therm Bea were also used in the form of aerosol. The aim of the test was to detect surface errors and narrow cracks that had not been identified at the time of visual inspection. Their intensity were measured by the Luxmeter of Testo 540. After checking the quality of the surfaces, the wheel was chip-machined by turning to the required dimensions. Subsequently, the machined surface of the newly formed layers was subjected to ultrasonic inspection with a Sonatest D70 (product Sonatest Ltd., Wolverton, UK) according to EN ISO 17640 [25]. Sono 600 gel was used as the binding medium. The defects were classified according to EN ISP 6520-1.

After the non-destructive inspection of the quality of the clads, samples were taken from the wheels by cutting to assess the quality of the clads by macrostructural and microstructural analysis. Macro-structural and microstructural analysis was carried out according to EN ISO 17639 [26] using Olympus VANOX-T (product Olympus, Tokyo, Japan) light microscopes and Keyence VHX 5000 (product Keyence, Mechelen, Belgium) and Leica WILD M3Z (product Leica Camera AG, Wetzlar, Germany) macroscopes on samples etched with 3% NITAL etchant. A very important factor in the formation of the functional layers is to mix the coating metal as little as possible with the underlying base material, but it is important that it is compactly bonded to the substrate layer. The experiment also assessed the hardness behavior in the different areas and the influence of the applied surfacing technology on the changes induced by the heat input to the material in the sub-surfacing area. The Vickers linear microhardness analyses were carried out in accordance with EN ISO 9015-1 [27] on an HPO 250 machine (product WPM LEIPZIG, Leipzig, Germany). HV30 tensioning was used. In technical practice, crane wheels are subjected to high surface pressure in an interaction with several types of wear. When assessing the interaction between wheel and rail, particular consideration must be given to the type of wear resulting from their mutual contact and movement. The dominant wear is adhesive wear. In particular, during starting and braking, there is intense friction between the surfaces. A secondary factor influencing the intensity of wear and the change in the type of wear is dirt. Impurities in the form of hard abrasive particles from the manufacturing process as well as corrosion products act as abrasives and also contribute significantly to the

degradation of functional wheel surfaces. In the experiments, we focused on the evaluation of tribological properties of newly formed surfaces under conditions of adhesive wear. The adhesive wear of the investigated materials was tested using AMSLER (product mpk-LUDWIG UG, Emsbüren, Germany) experimental testing, which allows testing materials with both planar and line contact. It allows dry testing of sliding pairs and also friction pairs with lubrication.

In our case, the adhesive wear was carried out under dry friction. The surfaces of the test specimens were cleaned with carbon tetrachloride (CCl_4) immediately before the experiment. Wheel discs of $18 \times 18 \times 15$ mm were taken from the wheels (Figure 5). The durability of the surface chip-treated coating of the coating was evaluated. The surface roughness of the evaluated surfaces was $R_a = 3.2 \mu\text{m}$ for all the specimens, as well as for the counter surface. As a rotating counter-piece, a disc of $\phi 35$ mm and 10 mm thickness with a $\phi 10$ mm hole for clamping in the testing machine was used, made of R260 rail material EN 13674-4. The bearing of the disc and the plate was adjusted to the pressure in the contact area by compressing the spring with a load of 1.5 kN. The steel disc was rotated at a speed of 200 rpm. The magnitude of adhesive wear of the materials was evaluated based on the weight changes of the test specimens at each stage of the experiment. The ex-position times of the specimens were chosen to be 30 s^{-1} , 60 s^{-1} and 120 s^{-1} . The weight losses were evaluated by weighing on a Radwag XA 220 (product RADWAG Headquarters, Radom, Poland) laboratory balance with a range of up to 200 g and an accuracy of 0.0001 g.

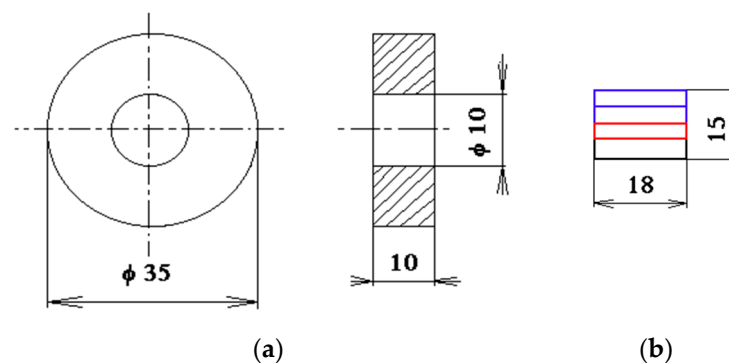


Figure 5. Schematic of the test specimens evaluated in the Amsler machine. (a) Rail material specimen; (b) cladded specimen.

3. Results

Results of the Visual Inspection of Claddings

On the basis of the visual inspection of the clads carried out in accordance with ISO EN ISO 17637 under 500 lux illumination, it can be stated that the functional parts of the wheel after chip machining did not show any surface defects. The wheel was machined to the required dimensions by turning. No chipping pores or cracks were identified that would classify the patterns as unsatisfactory. Visual inspection of the wheels was followed by capillary inspection. It was carried out in accordance with EN ISO 3452 (Figure 6). Its results confirmed the result of the visual inspection. The realized guides were free of surface defects. The residual developer (CaCO_3 coating) was cleaned from the wheel after the capillary inspection using Diffu-Therm BRE-S aerosol. The presence of internal defects was assessed by ultrasonic inspection in accordance with EN ISO 17640. The reflection method was used. The entire wheel circumference including the rims was analysed. The presence of internal defects in the flange or subflange layers was not observed.



Figure 6. Running wheel w03 during capillary check—outside of rim.

As part of the destructive inspection, the quality of the clad layers on the anterior metallographic cuttings was analyzed. The results of the microscopic observations are documented in Figures 7–16. After heat treatment, it had a sorbitic structure, which is documented in Figure 7. Due to the high carbon content, it is necessary to apply preheating during welding and cladding processes. The curved layer of the clad layer made with wire A1 is documented in Figure 8. It is a heat-treated bainitic–sorbitic structure. The presence of acicular ferrite and numerous predominantly globular inclusions was also noted. The transition of CL to IL and the well-defined orientation of the columnar grains as well as their size variation is noted in Figure 9. The transition of the IL to the basal material is shown in Figure 10. The microstructure of the clad layer of wheel 02 is recorded in Figure 11. It was a loose sorbitic structure with a characteristic dendritic arrangement and well-defined oriented grains. The aim of the innovation of the clad metal chemical composition was to achieve an increase in the proportion of hard carbide inclusions in the base matrix. The chemical composition of the additive material used and the chosen cladding parameters allowed for the production of a structure without significant carbide despite a significantly higher content of carbide additives (Cr 2.9% and Mo 0.9%) compared to round 01, which was one of the objectives. Possible massive carbide compounds could negatively affect the resulting strength properties of the layers under repeated cyclic loading at high pressures [28,29]. The transition of the cover layer to the interlayer was easily readable. It is documented in Figure 12. The interlayer had an annealed ferritic–pearlitic structure with the occurrence of acicular ferrite. The microstructure of the transition of the interlayer into the base material of wheel 02 is shown in Figure 13. The transition is easily legible. The presence of inclusions was noted in the base material, which was not analyzed. The microstructure of the clad metal made with the additive material marked C1 is shown in Figure 14. It was an annealed bainitic structure with an easily legible arrangement of columnar grains. The solidification process of the clads was easily readable. The crystallization of the grains broke through at a characteristic dihedral angle, which is documented in Figure 15. The microstructure of the interlayer was, as in round 02, composed of an annealed ferritic–pearlitic structure and also acicular ferrite. The transition of the interlayer into the base material was sharp (Figure 16). The transition region was easily readable. The thickness of the HAZ corresponded to the cladding technology used.

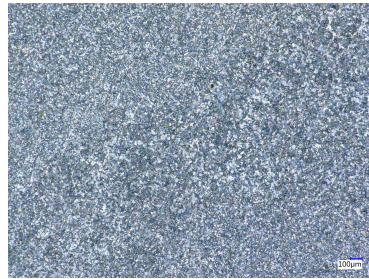


Figure 7. Wheel base material—heat-treated steel no. 1.0553.

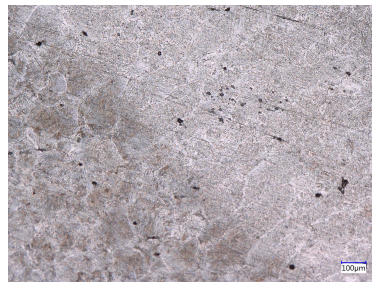


Figure 8. Microstructure of CL and transition to IL of wheel 01.

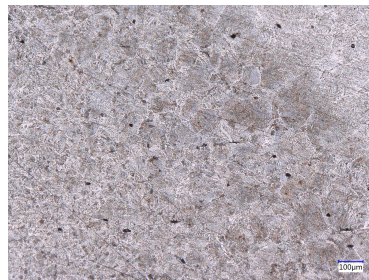


Figure 9. Microstructure of the CL to IL transition in wheel 01.



Figure 10. Microstructure of the IL to HAZ transition of round 01.



Figure 11. Microstructure of the CL clad of the wheel 02.

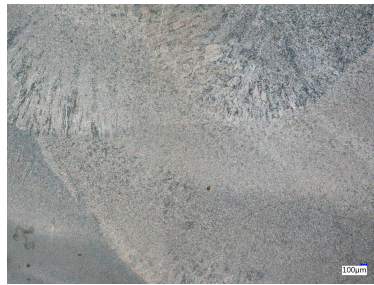


Figure 12. Microstructure of the CL to IL transition of the 02 wheel.

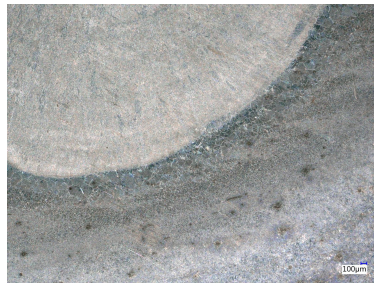


Figure 13. Transition IL to BM in wheel 02.



Figure 14. Microstructure of CL clad of the wheel 03.



Figure 15. Microstructure of the CL to IL transition of the wheel 03.

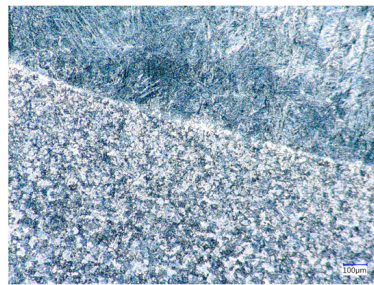


Figure 16. Transition IL to BM in wheel 03.

The presence of massive carbide inclusions was not observed in the microstructures of the cladding layers of rounds 02 and 03.

The results of the hardness evaluation are documented in the graph in Figure 17. Presented are the incremental values measured in lines on three samples from each wheel. Twenty-four indenter punctures were performed on each test lug. The first indentation was at a depth of 0.5 mm from the specimen surface, in the cover layer of the coating, and the last indentation was at a depth of 12 mm from the specimen surface, i.e., in the base material. Based on the measured values, it can be concluded that the maximum hardness values were exhibited by the clad in the cover layer made with C1 wire. An average hardness value of 461HV30 was measured at a depth of 0.5 mm. The maximum hardness value was also measured at a depth of 0.5 mm from the surface of the clad for the B1 wire. An average hardness of 358HV30 was measured in the cover layer. Among the evaluated additive materials used to produce the cover layers, the 317HV30 cladding layer showed the lowest average hardness at 1.5 mm depth for the cladding layer made with commercial A1 wire. The lowest average hardness values were measured in the interlayer area made with D1 wire, namely, 272HV30. These measured values were consistent with the chemical composition of the cladding wire used. The base material for all the wheels evaluated showed reasonable hardness values in the range 290HV30–282HV30.

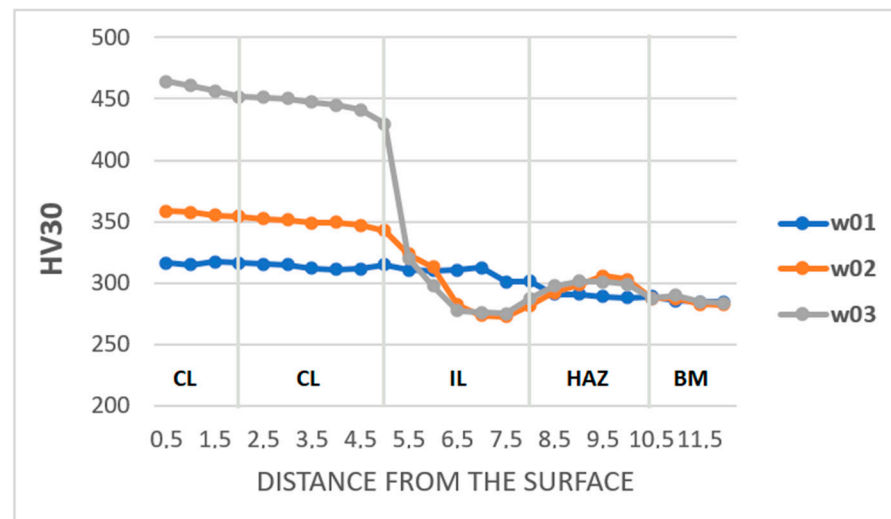


Figure 17. Measured average hardness values HV30 measured on clads from wheels. CL—covering layer; IL—inter layer, HAZ—heat-affected zone; BM—base material.

In the framework of the evaluation of the resistance of the newly formed layers to the action of tribodegradation factors, the research was focused on the evaluation of the influence of adhesive wear on functional surfaces. Five test specimens from each wheel were evaluated at the specified test time. One set of tribological pairs is documented in Figure 18. The resistance of the test specimens' surfaces was assessed based on their weight loss. The same surface quality was used for all friction pairs. The surface perimeter of the rollers was turned to a roughness of $R_a = 3.2 \mu\text{m}$. Similarly, the milled surfaces of the squares taken from the rolled wheels had a surface roughness evaluated that matched the chemical composition of the clad coat at a depth of 1 mm from the surface of the roll to a roughness of $R_a = 3.2 \mu\text{m}$. The roughness was checked prior to the test with a Mitutoyo SurfTest SJ 302 contact roughness tester produced Mitutoyo Corporation, Kanagawa, Japan. The tribological pair was contact machined. The measured average weight loss results are documented in the graph in Figure 19.



Figure 18. Tribological pairs after the 120 s^{-1} friction test.

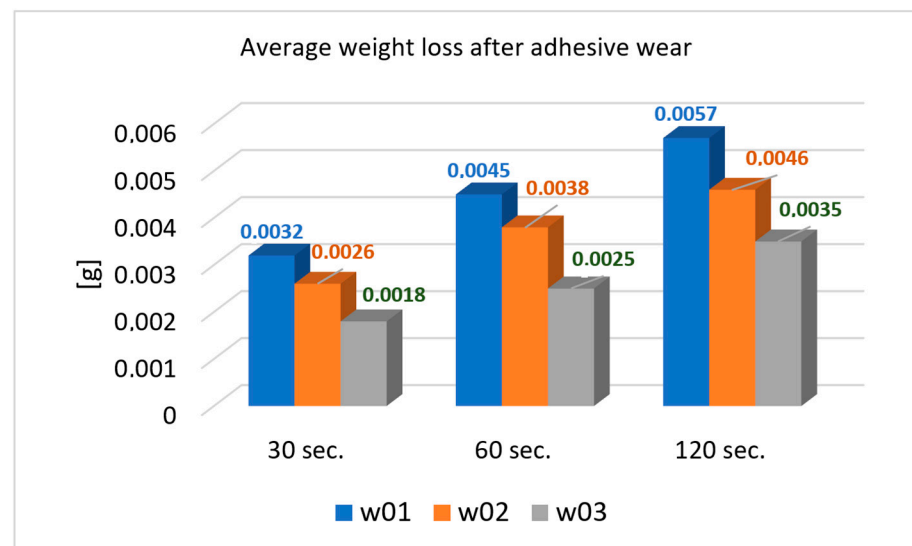


Figure 19. Average values weight loss samples after adhesive wear.

Prior to the test, the surface hardness at the point of contact of the tribological pair was measured on the surface of the roller of the rail material. The average surface hardness on the rollers was 216HV30. The average hardness measured on the A1 roll face was 315HV30. On the B1 clad, 358HV30 was measured, and on the C1 clad surfaces, an average hardness value of 465HV30 was measured. These values corresponded to the measured values presented in Figure 17.

Based on the results of the evaluation of the effect of adhesive wear during the selected times, it can be concluded that the surface with the clad made with C1 additive material showed the highest resistance to material removal. At time 30 s^{-1} , an average weight difference of 0.0018 g was recorded for the samples. At time 60 s^{-1} , it was 0.0025 g and at 120 s^{-1} exposure, it was 0.0035 g. Compared to the conventional type of additive material, which was a wire designated as A1 adhesive wear, a second newly developed wire designated as B1 also resisted adhesive wear better.

4. Discussion

This paper was written on the basis of a practical requirement to innovate the restoration processes for the functional surfaces of machine components under extreme stress, to

which mobile cranes undoubtedly belong. They are frequently used in the metallurgical industry, engineering enterprises, ports and transshipment plants. The frequency of their use and the weight of the goods they transport often make them an indispensable component; their collapse would stop the company that utilises them from functioning. For these reasons, great attention is paid to their operation and possibilities for their repair. In the framework of this research, the possibility of changing the chemical composition of long-used additive materials for the restoration of the functional surfaces of mobile crane wheels were verified. These surfaces include, in particular, the wheel circumference and the rims, which ensure the retention of the crane wheels on the rails. Mobile crane wheels are currently manufactured from various grades of steel. They are manufactured through casting, using mostly cast steel, but cast iron wheels can also be found. They are also produced as forgings. In our case, the base material used for the wheels was steel No. 1.0553. This is a carbon non-alloy steel. It has a high carbon content, which significantly impairs the possibility of repairing it using arc welding and cladding methods. It is these arc welding methods that are most suitable for restoring the functional surfaces of running wheels. It is also possible to renovate cast steel wheels by applying progressive energy beam methods, such as laser and plasma beams, but the economic aspect plays a significant role in the renovation process and, here, such progressive methods lose their suitability, as presented in the paper by Lewis, S.R. et al. [30]. For the given dimensions of the components, the most suitable renovation methods to apply are the processes of submerged arc cladding, cladding in protective gaseous atmospheres of with melting electrodes, self-shielded wires, etc. Local repairs can also be carried out through cladding using the GTAW or MMAW methods. In this paper, results showing the possibility of changing the conventionally used additive material used for automated submerged arc cladding, which has been designated as material A1, were presented. This additive material is predominantly used in renovations in three layers, without an intermediate layer formed by another type of additive material. However, the number of layers depends on the extent of damage to the wheel. The aim of the research was to verify the possibility of changing the chemical composition of the cladding wire in order to produce a compact, high-quality surfacing layer. The additional aims were to analyze the properties of these layers under laboratory conditions and to compare them with those of the commercially used type. Subsequently, the wheels were renovated using the new types of additive materials used in production plants, and they will be additionally subjected to operational tests in future. As new types of additive materials for the submerged cladding of the wheels, custom-made wires were produced, which were designated as B1 and C1. Their chemical composition differed compared to A1 wire mainly in their contents of carbide-forming elements such as Cr, Mo, Al and Ni. The Si content was also increased. The addition of these alloying elements led to the assumption of a resultant increase in the hardness of the functional layers and also an increase in the tribological resistance [31]. These assumptions were confirmed in the experiment. The cladding processes were carried out under approximately the same conditions as those that are currently implemented with A1 wire. However, a significant difference was the use of a sublayer under the clads made with new types of additive materials. Because of the expected increase in the hardness of the cover layers and the reduction in the plastic properties of the newly formed metal, an interlayer was applied which was formed with a low-alloyed wire type, designated as D1. This wire had significantly lower strength and hardness compared to the base material and also to the cladding materials B1 and C1. The purpose of this intermediate layer, called the cushion layer, was to improve the weldability conditions during the cladding of the cover layers, since the C content of its chemical composition was only minimal; given its mechanical properties, it was also expected to have a favourable effect when the wheels were under high-pressure conditions, which will be verified in the future operational tests. By increasing the proportion of carbide-forming additives in the new types of clads, the possibility of the formation of finely dispersed carbide particles of loosened sorbitol and loosened bainite in the casting structure was investigated.

As demonstrated using hardness measurements, these carbide particles increased the hardness of the functional part of the wheel by 40HV30 for the B1 wire and by 150HV30 for the C1 wire, compared to a clad made with A1 wire. However, the changes in chemical composition were most evident in the evaluation of the tribological properties of the flanges. In particular, C1 wire appeared to be a promising alternative to A1 wire. As was observed, the increased proportion of Cr and Mo in the structure, combined with the heat treatment of the rims, enabled the formation of the fine dispersed carbide, which strengthened the MC, delayed the microstructural recovery, and was important for improving the creep rupture strength of steel [32]. The popular Cr–Fe-rich carbide M_7C_3 grows easily and usually precipitates on the lath or block boundaries; this caused the migration of grain boundaries on the wheel and, therefore, shortened the time to the onset of creep acceleration [33,34].

The heat treatment of the wheels plays an important role in the renovation process. Due to the chemical composition of the base materials of the wheels (especially their high C contents, totalling 0.42–0.46%), it is necessary to ensure that all technological measures are consistently fulfilled. The preheating of the wheels is inevitable during the renovation process, as the required temperature to carry out cladding with subsequent reheating must be reached. Immediate heat treatment through annealing is recommended, due to the residual stresses concentrated in the cladding and sub-cladding area. The temperature rise in the annealing furnace must be continuous. The cooling of the wheels must also be carried out in accordance with the procedure presented. During the experiments, destruction of the cladding occurred in the case of the premature interruption of wheel preheating, the stacking of the wheels on the floor outside the furnace or on the hatch of the furnace and their subsequent placement in the cold furnace. After the heat treatment, it is advisable to place the wheels on stands, which allow the wheels to be hung by their centre hole, followed by uniform cooling around the circumference. Destruction of the clads may also occur due to uneven cooling caused by draughts in the hall. On the basis of the experiments carried out, it is possible to recommend C1 wire, and also B1 wire, for the renovation of wheels using the submerged arc cladding method.

5. Conclusions

The renovation of functional component surfaces is a topical issue at the moment. The rise in steel prices due to high demand is forcing many companies to look for solutions to extend the life of components and, thus, of the entire machine. On the basis of such a practical requirement, in cooperation with a manufacturer of additive materials, cladding wires with different chemical compositions were designed, the cladding parameters were proposed, the cladding process was implemented and the quality of the newly formed clad layers was evaluated using selected procedures. From these realized experiments, it was possible to define the following conclusions:

The additive materials used were designed in cooperation with their manufacturer to meet the renovation contractor's requirements for using the SAW (submerged arc welding) method for welding/cladding, specifically method No. 125 (ISO 4063)—submerged arc welding with tubular cored electrode. The cladding wires were made in the form of tubular wires. The newly developed wires (B1, C1) were, similarly to the conventional type of wire (A1), made with a diameter of 3.2 mm. Considering the dimensions of the additional materials, the same cladding parameters were used. The clads were made as a three-layer clad. Clads made of newly developed wires used an interlayer. For the conventional wire type, an interlayer was not used.

A very important factor in the renovation process of rolling wheels is the thermal treatment used during and immediately after the renovation process. Due to the chemical composition of the wheels, namely that of carbon steel no. 1.0553 used for casting, we used a preheating temperature of 150 to 200 °C, an interpass temperature at the same interval and reheating with a subsequent annealing process during the cladding process, to eliminate the formation of both cold and hot cracks. This was followed by even heating to a temperature of 800–840 °C. The heating was followed by cooling in the oven to 620 °C

for 2.5 h. After removing the wheels from the furnace, the wheels were cooled in the air. The heat treatment of crane wheels must take into account the materials used as well as the cladding technology used. The selected heat treatment procedures were also based on the research published by Korotkov, V.A. in [35] and Li, Y.K. et al. in [36], where, in addition to the hardness of the layers, they paid primary attention to minimizing residual stresses.

Based on the practical experience gained during the experiments, it can be concluded that the cooling process plays an important role in restoration. It must be uniform after the wheel has been drained. Placing the wheels on the cold ground, on stands in draughts, or leaning wheel parts against cold objects may cause the destruction of the clad layer.

The quality of the surfacing layers was evaluated using non-destructive testing. On the basis of this test's results, it can be stated that no surface defects were identified on any of the renovated wheels through visual and capillary inspection. Similarly, the presence of internal defects was not noted when inspected using ultrasound and the reflection method.

The structures of the individual strands were evaluated using light microscopy. For the overlays made with C1 and B1 wires, an annealed bainitic and an annealed sorbitic structure with a legible arrangement of columnar grains, respectively, was observed. The cover layer of the clad made by the additive material A1 had a structure formed by a heat-treated bainitic–sorbitic structure. The types of structures obtained were consistent with the structures described by Kharпов, A.A and Tanaskovic, D. et al., in their paper [37] on moving wheels, as well as in another paper by Kharпов, A.A and Tanaskovic, D. et al. [38].

The hardness assessment confirmed the assumptions about the influence of alloying additives on the resulting hardness. The increase in carbide-forming additives (Cr, Mo) in C1 wire resulted in an increase in hardness to 461HV30 in the cover layer of the clad, compared to 317HV30 for the cover layer clad made with conventional A1 wire. These hardnesses observed after heat treatment correspond approximately to the hardnesses published by Moshkbar Bakhshayesh in his paper [39]. He obtained the hardness of welds in high-alloy additives with a Cr content of 12–14%. Tempering martensite leads to a reduction in hardness from 418 to 351 HV0.3. The application of such high-alloy types of additives, if not necessary from the point of view of corrosion, unnecessarily increases the cost of the wires.

The results of the evaluation of the effect of the adhesion measure on the functional surfaces, evaluated on the basis of the weight losses of the test specimens, confirmed the positive effect of the chemical composition modification of the additive materials for the production of the cladding layers. Compared to the clads made with conventional A1 wire, the adhesion resistance of the clads made with C1 wire increased by 45%, and that of the clads made with B1 wire increased by 18%.

Research into the development of additive materials for the restoration of functional surfaces is ongoing. The properties of the newly developed claddings are assessed comprehensively, not only on the basis of experimental tests, but also on the basis of operational tests, which will contribute to the overall assessment of the suitability of the implementation of these innovative wire chemical compositions. These operational trials are ongoing. Future research will also be directed towards assessing the impact of a corrosive environment on the newly formed layers. As cranes are operated in aggressive corrosive environments, this may also contribute to intensifying tribodegradation processes and reducing wheel lifetimes.

Author Contributions: Conceptualization, J.V. and J.B. (Janette Brezinová); methodology, J.V. and P.H.; validation, P.H., P.P. and T.A.K.; formal analysis, J.B. (Janette Brezinová); investigation, J.B. (Jakub Brezina); resources, J.V., J.B. (Janette Brezinová) and P.H.; data curation, J.V. and P.P.; writing—original draft preparation, J.V. and P.H.; writing—review and editing, J.V. and J.B. (Janette Brezinová); visualization, P.P. and T.A.K.; supervision, J.V.; project administration, J.B. (Janette Brezinová); funding acquisition, J.B. (Jakub Brezina). All authors have read and agreed to the published version of the manuscript to the work reported.

Funding: This research was funded by the Ministry of Education, Science, Research and Sport of the Slovak Republic VEGA 1/0597/23 and the Slovak Research and Development Agency APVV-20-0303, KEGA 046TUKÉ-4/2022 and KEGA 018TUKÉ-4/2024.

Data Availability Statement: The original contributions presented in the study are included in the article; further inquiries can be directed to the corresponding author.

Conflicts of Interest: The authors declare no conflicts of interest.

References

1. Chovnyuk, Y.; Cherednichenko, P.; Kravchuk, V.; Ostapushchenko, O.; Kravchenko, I. Dynamic loads in elastic elements/ropes of construction cranes analysis and optimization. *Spat. Dev.* **2023**, *90*–107. [\[CrossRef\]](#)
2. Chen, K.; Zhou, H.; Shan, X. Rotation-Control Device for Construction Cranes with Nested PID Control. *Autom. Constr.* **2023**, *146*, 104704. [\[CrossRef\]](#)
3. Wang, R.D.; Zayed, T.; Pan, W.; Zheng, S.; Tariq, S. A System Boundary-Based Critical Review on Crane Selection in Building Construction. *Autom. Constr.* **2021**, *123*, 103520. [\[CrossRef\]](#)
4. Olearczyk, J.; Al-Hussein, M.; Bouferguène, A. Evolution of the Crane Selection and On-Site Utilization Process for Modular Construction Multilifts. *Autom. Constr.* **2014**, *43*, 59–72. [\[CrossRef\]](#)
5. Tran, Q.H.; Huh, J.; Nguyen, V.B.; Haldar, A.; Kang, C.; Hwang, K.M. Comparative Study of Nonlinear Static and Time-History Analyses of Typical Korean Sts Container Cranes. *Adv. Civ. Eng.* **2018**, *2018*, 2176894. [\[CrossRef\]](#)
6. Tang, G.; Shi, C.; Wang, Y.; Hu, X. Strength Analysis of the Main Structural Component in Ship-to-Shore Cranes under Dynamic Load. *IEEE Access* **2019**, *7*, 23959–23966. [\[CrossRef\]](#)
7. Krynke, M.; Mielczarek, K. Safety Management at the Design Stage of Rotation Node in Mobile Crane. *Syst. Saf. Hum. Tech. Facil. Environ.* **2022**, *4*, 116–127. [\[CrossRef\]](#)
8. Zhou, W.; Zhao, T.; Liu, W.; Tang, J. Tower Crane Safety on Construction Sites: A Complex Sociotechnical System Perspective. *Saf. Sci.* **2018**, *109*, 95–108. [\[CrossRef\]](#)
9. Li, A.; Zhao, Z. Crane Safety Assessment Method Based on Entropy and Cumulative Prospect Theory. *Entropy* **2017**, *19*, 44. [\[CrossRef\]](#)
10. Sodangi, M. Safety Risk Factors for Tower Cranes Used by Small and Medium-Scale Contractors on Construction Sites. *Int. J. Adv. Sci. Eng. Inf. Technol.* **2023**, *13*, 514. [\[CrossRef\]](#)
11. Im, S.; Park, D. Crane Safety Standards: Problem Analysis and Safety Assurance Planning. *Saf. Sci.* **2020**, *127*, 104686. [\[CrossRef\]](#)
12. Li, Y.; Wei, D. Checking Computation of Reliability for Traveling Skidding of Portal Crane. *J. Wuhan Univ. Technol. Transp. Sci. Eng.* **2006**, *30*, 417–420.
13. Lv, S.; Hu, X. Research on Performance Degradation Assessment and Abnormal Health Status Detection of Quayside Crane Lifting Gearbox Based on Information Fusion. *J. Mar. Sci. Eng.* **2023**, *11*, 1434. [\[CrossRef\]](#)
14. Kulka, J.; Mantic, M.; Fedorko, G.; Molnar, V. Analysis of Crane Track Degradation Due to Operation. *Eng. Fail. Anal.* **2016**, *59*, 384–395. [\[CrossRef\]](#)
15. Szpytko, J.; Duarte, Y.S. Technical Devices Degradation Self-Analysis for Self-Maintenance Strategy: Crane Case Study. *IFAC-PapersOnLine* **2021**, *54*, 729–736. [\[CrossRef\]](#)
16. Hassan, M.; Hussain, G.; Ilyas, M.; Ali, A. Delamination Analysis in Single-Point Incremental Forming of Steel/Steel Bi-Layer Sheet Metal. *Arch. Civ. Mech. Eng.* **2020**, *20*, 39. [\[CrossRef\]](#)
17. Kettler, M.; Zauchner, P.; Unterweger, H. Determination of Wheel Loads from Runway Cranes Based on Rail Strain Measurement. *Eng. Struct.* **2020**, *213*, 110546. [\[CrossRef\]](#)
18. Brezinová, J.; Viňáš, J.; Brezina, J.; Guzanová, A.; Maruschak, P. Possibilities for Renovation of Functional Surfaces of Backup Rolls Used during Steel Making. *Metals* **2020**, *10*, 164. [\[CrossRef\]](#)
19. Mortazavian, E.; Wang, Z.; Teng, H. Repair of Light Rail Track through Restoration of the Worn Part of the Railhead Using Submerged Arc Welding Process. *Int. J. Adv. Manuf. Technol.* **2020**, *107*, 3315–3332. [\[CrossRef\]](#)
20. EN 13674-4; Railway Applications—Track—Rail—Part 4: Vignole Railway Rails from 27 kg/m to, but Excluding 46 kg/m. iTeh Standards: Brussels, Belgium, 2019.
21. DIN 32522; Fluxes for Submerged Arc Welding—Designation—Technical Delivery Conditions. German Institute for Standardisation: Berlin, Germany, 1981.
22. EN ISO 17637; Non-Destructive Testing of Welds—Visual Testing of Fusion-Welded Joints. ISO: Brussels, Belgium, 2016.
23. EN ISO 6520-1; Welding and Allied Processes—Classification of Geometric Imperfections in Metallic Materials—Part 1: Fusion welding. ISO: Brussels, Belgium, 2008.
24. EN ISO 3452; Non-Destructive Testing—Penetrant Testing—Part 1: General Principles. ISO: Brussels, Belgium, 2023.
25. EN ISO 17640; Non-Destructive Testing of Welds—Ultrasonic Testing—Techniques, Testing Levels, and Assessment. ISO: Brussels, Belgium, 2019.
26. EN ISO 17639; Destructive Tests on Welds in Metallic Materials: Macroscopic and Microscopic Examination of Welds. ISO: Brussels, Belgium, 2023.

27. EN ISO 9015-1; Destructive Tests on Welds in Metallic Materials—Hardness Testing—Part 1: Hardness Test on Arc Welded Joints. ISO: Brussels, Belgium, 2011.
28. Zheng, Y.; Wang, F.; Li, C.; Li, Y.; Cheng, J.; Cao, R. Effect of Microstructure and Precipitates on Mechanical Properties of Cr–Mo–V Alloy Steel with Different Austenitizing Temperatures. *ISIJ Int.* **2018**, *58*, 1126–1135. [[CrossRef](#)]
29. Wu, T.; Ding, W.H.; Qi, C.; Sun, L.; Liu, T.W.; Pan, J.; Zhang, Z.Q. Influence of Carbide Morphology on Residual Stress of High Strength Steel during Tempering. *Cailiao Rechuli Xuebao/Trans. Mater. Heat Treat.* **2021**, *42*, 80–88. [[CrossRef](#)]
30. Lewis, S.R.; Lewis, R.; Fletcher, D.I. Assessment of Laser Cladding as an Option for Repairing/Enhancing Rails. *Wear* **2015**, *330–331*, 581–591. [[CrossRef](#)]
31. Studeny, Z.; Krbata, M.; Dobrocky, D.; Eckert, M.; Ciger, R.; Kohutiar, M.; Mikus, P. Analysis of Tribological Properties of Powdered Tool Steels M390 and M398 in Contact with Al₂O₃. *Materials* **2022**, *15*, 7562. [[CrossRef](#)]
32. Abe, F.; Horiuchi, T.; Taneike, M.; Sawada, K. Stabilization of Martensitic Microstructure in Advanced 9Cr Steel during Creep at High Temperature. *Mater. Sci. Eng. A* **2004**, *378*, 299–303. [[CrossRef](#)]
33. Abe, F.; Nakazawa, S.; Araki, H.; Noda, T. The Role of Microstructural Instability on Creep Behavior of a Martensitic 9Cr-2W Steel. *Metall. Trans. A* **1992**, *23*, 469–477. [[CrossRef](#)]
34. Janovec, J.; Svoboda, M.; Kroupa, A.; Výrostková, A. Thermal-Induced Evolution of Secondary Phases in Cr-Mo-V Low Alloy Steels. *J. Mater. Sci.* **2006**, *41*, 3425–3433. [[CrossRef](#)]
35. Korotkov, V.A. Surface Hardening Equipment. *Chem. Pet. Eng.* **2013**, *48*, 11–12. [[CrossRef](#)]
36. Li, Y.; Chen, J.; Lu, S. Residual Stress in the Wheel of 42CrMo Steel during Quenching. *Jinshu Xuebao/Acta Metall. Sin.* **2014**, *50*, 121–128. [[CrossRef](#)]
37. Khrapov, A.A.; Khripunov, V.M. Repair and a calculation-experimental method of determining the hardfacing conditions of crane wheels. *Weld. Prod. (Engl. Transl. Svarochnoe Proizv.)* **1986**, *33*, 9–11.
38. Tanskovič, d.; Sedmak, S. The Effect of Cracks on Stress State in Crane Wheel Hard-Surface under Contact Loading. *Teh. Vjesn.—Tech. Gaz.* **2017**, *24*, 169–175. [[CrossRef](#)]
39. Moshkbar Bakhshayesh, M.; Farzadi, A.; Kalantarian, R.; Zargarzadeh, A. Evaluation of Crane Wheels Restored by Hardfacing Two Distinct 13Cr-4Ni Martensitic Stainless Steels. *J. Mater. Res. Technol.* **2023**, *26*, 6067–6083. [[CrossRef](#)]

Disclaimer/Publisher’s Note: The statements, opinions and data contained in all publications are solely those of the individual author(s) and contributor(s) and not of MDPI and/or the editor(s). MDPI and/or the editor(s) disclaim responsibility for any injury to people or property resulting from any ideas, methods, instructions or products referred to in the content.